HHS Public Access

Author manuscript

Nature. Author manuscript; available in PMC 2013 February 22.

Published in final edited form as:

Nature. 2012 August 23; 488(7412): 522–526. doi:10.1038/nature11287.

A restricted cell population propagates glioblastoma growth following chemotherapy

Jian Chen[1], **Yanjiao Li**[1], **Tzong-Shiue Yu**[1,2,4], **Renée M. McKay**[1], **Dennis K. Burns**[3], **Steven G. Kernie**[1,2,4], and **Luis F. Parada**[1,*]

[1]Department of Developmental Biology & Kent Waldrep Center for Basic Research on Nerve Growth and Regeneration, University of Texas Southwestern Medical Center, Dallas, Texas 75390-9133, USA

[2]Department of Pediatrics, University of Texas Southwestern Medical Center, 5323 Harry Hines Blvd., Dallas, TX 75390

[3]Department of Pathology, University of Texas Southwestern Medical Center, 5323 Harry Hines Blvd., Dallas, TX 75390

Abstract

Glioblastoma multiforme (GBM) is the most common primary malignant brain tumor, with a median survival of about one year[1]. This poor prognosis is due to therapeutic resistance and tumor recurrence following surgical removal. Precisely how recurrence occurs is unknown. Using a genetically-engineered mouse model of glioma, we identify a subset of endogenous tumor cells that are the source of new tumor cells after the drug, temozolomide (TMZ), is administered to transiently arrest tumor growth. A *Nestin-ΔTK-IRES-GFP* (*Nes-ΔTK-GFP*) transgene that labels quiescent subventricular zone adult neural stem cells also labels a subset of endogenous glioma tumor cells. Upon arrest of tumor cell proliferation with TMZ, pulse-chase experiments demonstrate a tumor re-growth cell hierarchy originating with the *Nes-ΔTK-GFP* transgene subpopulation. Ablation of the GFP+ cells with chronic ganciclovir administration significantly arrested tumor growth and combined TMZ-ganciclovir treatment impeded tumor development. These data indicate the existence of a relatively quiescent subset of endogenous glioma cells that are responsible for sustaining long-term tumor growth through the production of transient populations of highly proliferative cells.

Keywords

tumor hierarchy; cancer stem cells; cell ablation; glioma; ganciclovir

*Correspondence: Luis F. Parada, Ph.D. luis.parada@utsouthwestern.edu, Tel: 214-648-1822, Fax: 214-648-1960.

[4]Present address: Department of Pathology and Cell Biology, Columbia University, New York, NY

Author Contributions

J.C. and Y.L. performed the experiments. T-S.Y. and S.K.G. contributed vital reagents. J.C. and L.F.P. designed the experiments. J.C., R.M.M., D.B., and L.F.P. analysed the data. J.C., R.M.M. and L.F.P. wrote the paper.

We have extensively studied a series of mouse strains harboring conditional alleles of the tumor suppressors NF1, p53 and Pten, that spontaneously develop malignant gliomas with 100% penetrance, and have identified the source cells of these tumors as deriving from the subventricular zone (SVZ)[2–4]. Thus, we proposed that adult neural stem cells (NSCs) are the likely source of these tumors[2]. We wished to determine whether a *Nestin-ΔTK-IRES-GFP* (*Nes-ΔTK-GFP*) transgene[5], originally devised to mark adult NSCs, would also mark endogenous glioma cells. Elements of the nestin gene can drive transgene expression specifically in adult NSCs[2, 5] (Fig. 1a). The transgene also harbors a cassette containing a modified version of the herpes simplex virus thymidine kinase (ΔTK) allowing for temporally regulated ablation of dividing neural progenitors by systemic ganciclovir (GCV) administration, and an IRES-GFP cassette to mark *Nes-ΔTK*-expressing cells in the absence of GCV. The *Nes-ΔTK-GFP* transgenic mice showed the expected expression in both glial fibrillary acidic protein (GFAP)-positive adult NSCs and early doublecortin (DCX)-positive neural progenitor cells (NPCs) in the major adult NSC niche: the SVZ of the lateral ventricle (Fig. 1b, c). To validate that the GCV-activated *Nes-ΔTK-GFP* transgene could effectively eliminate endogenous neural stem/progenitor cells, one-month-old transgenic mice were treated with GCV for two weeks. In control mice, the rostral migratory stream (RMS), formed by NPCs migrating from the SVZ to the olfactory bulb, is visualized by Nissl staining. In contrast, the RMS was severely diminished in *Nes-ΔTK-GFP* mice after GCV treatment (Fig. 1b, bottom panel). Consistent with this observation, DCX immunostaining indicated absence of NPCs in the SVZ of GCV-treated *Nes-ΔTK-GFP* animals (Fig. 1c, bottom panel). Since in the presence of GCV, HSV-TK targets only proliferating cells, the GFAP-positive NSCs that remained quiescent were unaffected, although they also express the transgene as indicated by GFP (Fig. 1c, bottom panel). Thus, our *Nes-ΔTK-GFP* transgene is specifically expressed in SVZ quiescent and proximal progenitor cells and chronic GCV administration effectively blocks neurogenesis by ablating quiescent cells as they enter the cell cycle.

We bred the *Nes-ΔTK-GFP* transgene into *hGFAP-Cre;NF1$^{f/+}$;P53$^{f/f}$;PTEN$^{f/+}$* (*Mut7*) glioma-prone mice[3]. *Mut7* mice develop malignant glioma, with full penetrance, by somatic deletion of three of the most frequently mutated tumor suppressors in GBM: p53, NF1 and Pten[7]. All *Mut7;Nes-ΔTK-GFP* mice also developed gliomas and we observed only a subset of tumor cells expressing GFP (*Nes-ΔTK-GFP* positive; Fig. 1d, e). These cells also co-expressed the neural stem cell marker Sox2 (not shown). We next examined tumor cell proliferation and found that *Mut7;Nes-ΔTK-GFP* tumors exhibited a significant proportion of Ki67-positive/GFP-negative cells, and conversely, the subset of GFP-positive tumor cells rarely co-stained for Ki67 (Fig. 1e, f). These data indicate that most transgene GFP-positive tumor cells are relatively quiescent in comparison to a highly proliferative (Ki67+) subpopulation reminiscent of the SVZ where GFP-positive stem cells are quiescent compared to GFP-negative progenitors (Fig. 1c). Furthermore, as in wild type mice, where the *Nes-ΔTK-GFP* transgene does not affect SVZ neurogenesis in the absence of GCV administration (Fig. 1b, c), introduction of the transgene into the *Mut7* genetic background did not impact tumor development or enhance survival (Fig. 1g). Like *Mut7* mice, *Mut7;Nes-ΔTK-GFP* mice developed malignant glioma with 100% penetrance and with similar kinetics (Fig. 1g, h).

TMZ is a DNA alkylating agent that is currently the primary chemotherapy agent for GBM patients[6] as it has transient tumor growth arrest properties. We found that TMZ eradicates proliferative cells in the endogenous murine gliomas. TMZ was administered over several days to tumor-bearing mice followed by BrdU injection two hours after final treatment, and the mice sacrificed two hours thereafter (Fig. 2a). The TMZ-treated mice exhibited dramatic reduction of BrdU incorporation in both the tumors and NSC niches of TMZ-treated mice (Fig. 2b, c). Similar to treated glioma patients following TMZ treatment, the murine tumors reinitiated cell division and growth. Thus, TMZ targets proliferating cells but tumor recurrence is inevitable. To examine the details of tumor recurrence, we traced the first wave of tumor cell proliferation following completion of the drug regimen on tumor-bearing mice by pulse-chase using the BrdU analogs CldU and IdU. CldU and IdU were injected one day and three days, respectively, after the final TMZ injection (Fig. 2d). Given the variable but relatively low proportion of GFP-positive cells in all tumors (Fig. 1d, e), we reasoned that if cell proliferation reinitiated randomly in tumor cells after TMZ treatment, then the number of GFP-positive cells that would incorporate CldU and/or IdU should be low to insignificant. However, if renewed tumor cell proliferation was hierarchical and derived from the GFP-positive cells, a biased incorporation of nucleotide analogs into the relatively small GFP-positive cohort of tumor cells would result. Examination of tumor sections with IHC revealed that the large majority of cells incorporating CldU and IdU after relatively short chases also contained GFP expression (Fig. 2e, GFP% in CldU+ population = 77±14, GFP% in IdU+ population = 83±10). Moreover, IdU-positive cells retained both GFP and CldU, indicating that following TMZ eradication of a majority of pre-existing proliferating tumor cells, the re-emergent population of proliferating cells derived from *Nes*-Δ*TK*-*GFP*-expressing cells and not from random tumor or other specific subsets of cells (Fig. 2e, CldU % in IdU+ population=86±9). When the second, IdU, pulse was prolonged to a seven day chase following CldU pulse, most IdU cells double-labeled for CldU (85±7%) but lost GFP expression (Supplementary Fig. 1a–c). Thus, as in the normal SVZ stem cell niche, over time, the GFP-expressing glioma cell population gives rise to cells that progressively lose stem cell properties (i.e. nestin expression and relative quiescence) and concomitantly shut down the *Nes*-Δ*TK*-*GFP* transgene (Supplementary Fig. 1c, d). Using endogenous lineage tracing of renewed cell division within tumors, we have identified the relatively quiescent *Nes*-Δ*TK*-*GFP*-expressing tumor cells as the primary source of proliferating and eventually non-dividing tumor cell derivatives (Supplementary Fig. 1c, d). In addition, the data show that in our endogenous glioma models, TMZ targets the proliferating derivatives but not the GFP+ quiescent cells.

One prediction would be that eradication of the *GFP*-positive cells in the endogenous tumors should significantly decrease appearance of new dividing tumor cells. We tested this prediction at two stages: early endogenous tumor development and advanced tumor development. First, *Mut7;Nes*-Δ*TK*-*GFP* mice were treated with GCV beginning at eight weeks of age – the earliest time of detectable pre-tumorigenic anomalies[3]. To capture most quiescent GFP-positive cells in a dividing state, GCV treatment lasted for ten weeks, requiring three osmotic minipump placement surgeries that unfortunately were accompanied by complications resulting in significant variance of drug delivery. Drug delivery efficacy was qualitatively measured by examination of the normal stem cell niche response to drug

(Fig. 1b, c) as manifested by residual RMS (Supplementary Fig. 2a). Accordingly, tumor incidence varied from mouse to mouse, with some perishing early with large tumors. However, as a group, the GCV-treated cohort showed a clear survival advantage (Fig. 3a). After ten weeks of treatment, the only surviving mice were among those treated with GCV (Supplementary Fig. 2b), and analysis of their brains revealed only low-grade lesions (Supplementary Fig. 2c). When GCV was effectively delivered, survival was substantially prolonged and tumor progression was severely impaired. Thus, elimination of *Nes*-Δ*TK-GFP*-positive cells at early/pretumorigenic stages prevents development of high-grade gliomas.

A second GCV regimen was commenced in ten-week-old tumor-bearing mice. Most ten-week-old *Mut7* mice do not show neurological symptoms yet histological examination of large cohorts showed that all mice harbor astrocytoma of differing grades (Supplementary Fig. 3). We subjected ten-week-old *Mut7;Nes*-Δ*TK-GFP* or *Mut7* mice to GCV or saline for two months. GCV treatment of *Mut7;Nes*-Δ*TK-GFP* mice improved survival by approximately thirty days compared to saline control, while neither treatment was effective in improving survival of *Mut7* mice (Fig. 3b). Consistent with this, GFP and endogenous nestin double-immunostaining showed that GFP-positive cells were successfully eliminated in gliomas of *Mut7;Nes*-Δ*TK-GFP* mice following prolonged GCV treatment (Fig. 3c).

The residual tumors in these tumor-bearing *Mut7;Nes*-Δ*TK* mice treated with GCV beginning at 10 weeks of age did not have the classic glioma feature of invasiveness but instead were circumscribed with well defined boundaries (Fig. 3d, e, Supplementary Fig. 2d, e). Although the *Mut7;Nes*-Δ*TK-GFP* transgene is only expressed in a subset of cells in the untreated tumor (Fig. 1e), tumors in GCV-treated *Mut7;Nes*-Δ*TK* mice showed a marked reduction of Ki67-positive cells and stem cell markers (Fig. 3e–g). These data further support the hypothesis that chronic GCV administration progressively ablates the relatively quiescent GFP+ tumor cell population and the remaining GFP- tumor cells eventually exhaust their proliferative and infiltrative potential.

The HSV-TK system has been widely used as a method to induce endogenous cell suicide. A potentially confounding phenomenon is the “bystander effect” whereby HSV-TK-expressing cells not only commit suicide in the presence of GCV, but can also induce the death of neighboring non-TK-expressing cells[7]. However, several NSC-specific HSV-TK-expressing transgenic mice have been reported and no bystander effect has been described[8–11]. To examine whether tumor development was appreciably impaired by the bystander effect, we turned to transplantation assays.

We first determined whether GCV treatment would also blunt *Mut7;Nes*-Δ*TK-GFP* tumor growth in a transplantation assay. Primary gliomas from *Mut7;Nes*-Δ*TK-GFP* and *Mut7* mice were dissociated and directly injected subcutaneously into nude mice in the presence of continuous GCV or saline treatment (Supplementary Fig. 4a). Neither GCV nor saline affected the tumor growth of *Mut7*-derived cells (Supplementary Fig. 4b). In contrast, similar to a previous report[12], mice transplanted with *Mut7;Nes*-Δ*TK* tumor cells and then treated with GCV developed significantly smaller tumors that appeared poorly vascularized compared to saline-treated controls (Supplementary Fig. 4c–f). Thus, the *Mut7* tumor cells

transplant efficiently in immunocompromised mice, and, as in the endogenous setting (Fig. 3), GCV treatment severely impairs tumor development following transplantation. To test for bystander effect, we transduced primary *Mut7* cells with a lentivirus harboring either a control RFP cassette or an HSV-TK cassette (Supplementary Fig. 5a). Mixed ratios of the two cell populations were injected subcutaneously into nude mice and allowed to seed tumors for four weeks after which GCV was administered for two weeks (Supplementary Fig. 5b). The data indicate that the presence of a 10%, 20%, or 50% initial ratio of TK-expressing tumor cells did not impair tumor development of the non-TK-expressing cells in the presence of GCV (Supplementary Fig. 5c, d). In the extreme case when equal numbers of TK positive (10^5) and TK negative (10^5) cells were injected compared to 10^5 TK negative cells alone, tumor development was equivalent in both cohorts demonstrating that GCV toxicity to 50% of the tumor cells did not extend into the TK-negative tumor cell population (Supplementary Fig. 5c, d). In our endogenous tumors, such a bystander effect would require the relatively rare *GFP+* tumor-propagating cells to be widely toxic to have a significant paracrine effect on tumor properties. Instead, these studies indicate that GCV administration does not have an appreciable effect on cells outside those expressing the TK gene, consistent with other recently reported studies[8–12]. We conclude that eradication of the *Mut7;Nes-ΔTK-GFP* endogenous tumor cells via GCV treatment effectively disrupts the continued production of tumor cells as predicted from the preceding data.

Despite effective depletion of GFP-expressing tumor-propagating cells with GCV treatment, a significant residual tumor mass remained (Fig. 3d). We therefore attempted a therapeutic strategy to eliminate both the rapidly proliferating tumor cells and the quiescent GFP+ cells, by sequentially administering TMZ and GCV, respectively (Fig. 4a, b). Initially it appeared that this regimen did not prolong survival beyond that of GCV treatment alone (Fig. 4c). However, examination of the brains of the sequentially treated mice revealed only vestigial tumors in the dorsal brain that showed no transgene-GFP expression, indicating effective depletion (Fig. 4d). The cellular density of the residual TMZ/GCV-treated tumors was lower than that of tumors at the beginning of treatment (10 weeks), indicating a statistically significant reduction in tumor bulk. This contrast was significantly enhanced when treated tumors were compared to untreated control tumors (Fig. 4e), which manifested in a spectrum of survival time from 12 to 16 weeks. Thus, the combined treatment had dramatic inhibitory effects on dorsal tumor growth in these mice.

We were puzzled that TMZ/GCV treatment did not significantly prolong survival beyond the GCV-only treated mice where residual circumscribed tumor mass remained (Fig. 3d, e, Supplementary Fig. 2d, e). Analysis of the TMZ/GCV-treated brains revealed that despite the dramatic inhibition of original tumor growth, these mice developed novel tumors in the ventral brain region. Six of seven TMZ/GCV-treated mice showed tumors in the brain stem region, whereas gliomas in untreated *Mut7* mice, and their remnants in the successfully treated mice are predominantly located in the dorsal/midbrain (Supplementary Fig. 6a). Examination of the TMZ/GCV-resistant hindbrain tumors revealed high endogenous nestin protein but no GFP expression (SupplementaryFig. 6b,c). We also searched archived material and found that a small percentage of *Mut7* brains harbored both dorsal and ventral tumors that we now appreciate were independently arising and not extensions of the dorsal

tumors. Appearance of ventral tumors in the presence of GCV indicates an inactive *Nes-ΔTK-GFP* transgene, and direct examination of untreated *Mut7;Nes-ΔTK-GFP* mice demonstrated that the *Nes-ΔTK-GFP* transgene was indeed silent (Supplementary Fig. 6b,e).

We next examined the expression of tumor markers in these hindbrain tumors. In contrast to typical *Mut7* or *Mut7;Nes-ΔTK-GFP* gliomas, all ventral tumors in the TMZ/GCV group showed low levels of endogenous GFAP but relatively high levels of S100B (Supplementary Fig. 6c and data not shown). Seven of eleven tumors in the ventral and brain stem region of GCV-treated mice (GCV alone or TMZ & GCV) showed histopathological features of oligodendroglioma (Supplementary Fig. 7a–c) including high PDGFRA levels (Supplementary Fig. 7d). This is in contrast to the pure astrocytic tumors typically observed in this mouse model in the absence of TMZ/GCV. Thus, these data indicate that the ventral tumors that become evident after TMZ/GCV treatment are oligoastrocytic, independently arising, and distinct from the dorsal tumors. Such tumors were recently described in *Mut3* mice[13] and the source was reported to be oligodendroglial progenitors. We are currently further characterizing these tumors.

Our *Nes-ΔTK-GFP* transgene labels SVZ stem cells and, fortuitously, a specific subset of GBM cells that possesses many features proposed for cancer stem cells (CSCs). The CSC hypothesis holds that some tumors are composed of a hierarchical cadre of cells of which only a subset retains both self-renewal and differentiation capacity[14]. In this model, only CSCs have the capacity to sustain tumor growth and are responsible for recurrence after therapy fails.

The current standard for evaluating whether solid tumors contain CSCs is an *ex-vivo* limiting dilution tumorigenic transplantation assay into immunodeficient animals[14]. However, controversy regarding the presence and frequency of solid tumor CSCs remains, likely a reflection of the variability that accompanies such assays[15–18]. Our study identifies a putative endogenous glioma stem cell located at the apex of a cellular hierarchy in tumor maintenance and recurrence following chemotherapy (Fig. 4a). Continued evaluation of these cells and their properties, including isolation and genetic lineage tracing, may shed important insight into novel therapeutic targets for this intractable disease.

Methods Summary

Mice

All mice were maintained on a mixed 129SvJ/C57BL/6/B6CAB background. *Mut7* and *Mut7;Nes-ΔTK* mice were obtained by crossing male *hGFAP-Cre;P53$^{flox/flox}$* mice with female *NF1$^{flox/flox}$;P53$^{flox/flox}$;Pten$^{flox/flox}$;Nes-ΔTK* mice. Genotyping for *Mut7* mice was performed as reported previously[3].

In vivo chemical administration

Stock CldU (Sigma) and BrdU (Sigma) were dissolved in PBS at a concentration of 8.5 mg/ml and 10 mg/ml, respectively. 11.5 mg/ml IdU (MP Biomedicals) solution was made fresh each time[19]. To label dividing cells, 5 ml/kg stock solution was injected intraperitoneally each time according to the experimental design. Ganciclovir (GCV)

(Cytovene-IV, Roche Pharmaceuticals) treatment was performed as described[5]. For initial characterization of *Nes*-Δ*TK-GFP* mice, 1-month-old *Nes*-Δ*TK-GFP* or control mice were administered GCV (300 mg/kg/d) or PBS via osmotic minipump (Model 2002, 0.5 μl/h, Alzet) for 2 weeks. For treatment starting from 8 week or 10 weeks, 150 mg/kg/d GCV or PBS was delivered through osmotic minipump (Model 2004, 0.25 μl/h, Alzet); pumps were surgically removed and replaced every 4 weeks based on the experimental requirement. Temozolomide (TMZ) (Sigma) was dissolved in DMSO and injected intraperitoneally at a dose of 82.5 mg/kg/d for five days. For the combinational therapy group, mice were first treated with TMZ for five days and then osmotic minipumps with GCV were implanted 2 days after the last TMZ injection.

Histology and Immunohistochemistry

Mice were perfused and brains were processed as described earlier[2]. Paraffin brain H&E sections (5 μm) were reviewed by J.C. and D.K.B independently. Tumor type and grades were determined by D.K.B. 14 μm cryostat sections were used for GFP/CldU/IdU staining following reported methods[19]. Primary antibodies were used against GFAP (DAKO, 1:2000), Olig2 (Millipore, 1:1000), Sox2 (Millipore, 1:5000), Nestin (BD Biosciences, 1:200), CD44 (BD Biosciences, 1: 75), GFP (Rockland, 1:200, Aves Lab, 1:500), BrdU/IDU (BD Biosciences, 1:100), BrdU/CldU (AbD Serotec,1:500), Ki67 (Novacastra, 1:1000), PDGFRα (Santa Cruz, 1:200). Horseradish peroxidase-based Vectastain ABC Kit (Vector Laboratories) or Cy2/Alexa-488, C3/Alexa555, Cy5-labeled secondary antibodies (Jackson Labs, Invitrogen) were used to visualize the primary antibody staining.

Methods

Mice

All mouse experiments were approved by and performed according to the guidelines of the Institutional Animal Care and Use Committee of the University of Texas Southwestern Medical Center at Dallas. All mice were maintained on a mixed 129SvJ/C57BL/6/B6CAB background. *Mut7* and *Mut7;Nes*-Δ*TK* mice were obtained by crossing male *hGFAP-Cre;P53*$^{flox/flox}$ mice with female *NF1*$^{flox/flox}$*;P53*$^{flox/flox}$*;Pten*$^{flox/flox}$*;Nes*-Δ*TK* mice. Genotyping for *Mut7* mice was performed as reported previously[3].

In vivo chemical administration

Stock CldU (Sigma) and BrdU (Sigma) were dissolved in PBS at a concentration of 8.5 mg/ml and 10 mg/ml, respectively. 11.5 mg/ml IdU (MP Biomedicals) solution was made fresh each time[19]. To label dividing cells, 5 ml/kg stock solution was injected intraperitoneally each time according to the experimental design. Ganciclovir (GCV) (Cytovene-IV, Roche Pharmaceuticals) treatment was performed as described[5]. For initial characterization of *Nes*-Δ*TK-GFP* mice, 1-month-old *Nes*-Δ*TK-GFP* or control mice were administered GCV (300 mg/kg/d) or PBS via osmotic minipump (Model 2002, 0.5 μl/h, Alzet) for 2 weeks. For treatment starting from 8 week or 10 weeks, 150 mg/kg/d GCV or PBS was delivered through osmotic minipump (Model 2004, 0.25 μl/h, Alzet); pumps were surgically removed and replaced every 4 weeks based on the experimental requirement. Temozolomide (TMZ) (Sigma) was dissolved in DMSO and injected intraperitoneally at a

dose of 82.5 mg/kg/d for five days. For the combinational therapy group, mice were first treated with TMZ for five days and then osmotic minipumps with GCV were implanted 2 days after the last TMZ injection.

Histology and Immunohistochemistry

Mice were perfused and brains were processed as described earlier[2]. Paraffin brain H&E sections (5 μm) were reviewed by J.C. and D.K.B independently. Tumor type and grades were determined by D.K.B. 14 μm cryostat sections were used for GFP/CldU/IdU staining following reported methods[19]. Primary antibodies were used against GFAP (DAKO, 1:2000), Olig2 (Millipore, 1:1000), Sox2 (Millipore, 1:5000), Nestin (BD Biosciences, 1:200), CD44 (BD Biosciences, 1: 75), GFP (Rockland, 1:200, Aves Lab, 1:500), BrdU/IDU (BD Biosciences, 1:100), BrdU/CldU (AbD Serotec,1:500), Ki67 (Novacastra, 1:1000), PDGFRα (Santa Cruz, 1:200). Horseradish peroxidase-based Vectastain ABC Kit (Vector Laboratories) or Cy2/Alexa-488, C3/Alexa555, Cy5-labeled secondary antibodies (Jackson Labs, Invitrogen) were used to visualize the primary antibody staining. Images were taken using optical, fluorescence and confocal microscopy (Olympus and Carl Zeiss) and assembled in Adobe Illustrator (Adobe Systems Incorporated).

Temozolomide, BrdU analogs, and pulse chase experiments

To determine TMZ efficiency, 10- to 11-week-old *Mut7* mice were first injected intraperitoneally with 82.5 mg/kg/d TMZ for 5 days. 50 mg/kg BrdU was injected 2 hours after the final TMZ administration and mice were perfused 2 hours after BrdU injection. The brain was then paraffin-processed and cut into 5 μm-thick slices. H&E staining was performed every 70 μms to identify tumor location. Adjacent tumor sections were selected for GFAP and BrdU co-immunostaining.

For the short term CldU chase experiments, 10- to 11-week-old *Mut7;Nes*-Δ*TK* mice were first treated with TMZ for 5 days. A total of three doses of CldU were injected, with 2-hour intervals, the day after the final TMZ injection. A single dose of IdU was then injected 3 days after the final TMZ injection. For the long term CldU chase experiments, 10- to 11-week-old *Mut7;Nes*-Δ*TK* mice were first treated with TMZ for 5 days. CldU was injected 3 times a day, with 2-hour intervals, for 3 days after the final TMZ injection. A single dose of IdU was then injected 7 days after the final TMZ injection. Mice were perfused 2 hours after the IdU injection and the brains cryoprotected in 30% sucrose, embedded in OCT, and cut into 14 μm-thick frozen sections. GFAP and Ki67 co-immunostaining was performed every 140 μms to locate the tumor area. Adjacent sections were selected for GFP/CldU/IdU triple immuno-fluorescence staining.

Quantification

Because of the heterogeneous nature of the tumors, cell density, Ki67-index and BrdU-positive cell percentage were quantified using the highest staining area[1]. Briefly, staining was checked under low-magnification and the highest staining area was identified. The area was viewed at 200X in three continuous 5μm-thick sections and positive cells counted using the measured parameters.

For quantification of GFP/CldU/IdU triple staining, tumor areas with at least one CldU-positive cell were selected, and an 8 μm Z-stack image was scanned and constructed using confocal microscopy (Olympus and Carl Zeiss). A total of ten different areas within each tumor was imaged and subjected to quantification.

Supplementary Material

Refer to Web version on PubMed Central for supplementary material.

Acknowledgments

The authors thank Steven McKinnon, Alicia Deshaw, Linda McClellan, Shawna Kennedy and Patsy Leake for technical assistance, and Parada Lab members for helpful suggestions and discussion. CldU and IdU preparation and staining protocol was kindly provided by Dr. Daniel A. Peterson at Rosalind Franklin University. This work was supported by grants awarded to SGK (RO1 NS048192-01) and to LFP by the Goldhirsh Foundation, the James S. McDonnell Foundation (JSMF-220020206), CPRIT (RP 100782), and the NIH (R01 CA131313). LFP is an American Cancer Society Research Professor.

References

1. Chen J, McKay RM, Parada LF. Malignant glioma: lessons from genomics, mouse models, and stem cells. Cell. 2012; 149:36–47. [PubMed: 22464322]
2. Alcantara Llaguno S, et al. Malignant astrocytomas originate from neural stem/progenitor cells in a somatic tumor suppressor mouse model. Cancer Cell. 2009; 15:45–56. [PubMed: 19111880]
3. Kwon CH, et al. Pten haploinsufficiency accelerates formation of high grade astrocytomas. Cancer Res. 2008; 68:1–9.
4. Zhu Y, et al. Early inactivation of p53 tumor suppressor gene cooperating with NF1 loss induces malignant astrocytoma. Cancer Cell. 2005; 8:119–30. [PubMed: 16098465]
5. Yu TS, et al. Traumatic brain injury-induced hippocampal neurogenesis requires activation of early nestin-expressing progenitors. J Neurosci. 2008; 28:12901–12. [PubMed: 19036984]
6. Stupp R, et al. Radiotherapy plus concomitant and adjuvant temozolomide for glioblastoma. N Engl J Med. 2005; 352:987–96. [PubMed: 15758009]
7. Ishii-Morita H, et al. Mechanism of 'bystander effect' killing in the herpes simplex thymidine kinase gene therapy model of cancer treatment. Gene Ther. 1997; 4:244–51. [PubMed: 9135738]
8. Garcia AD, et al. GFAP-expressing progenitors are the principal source of constitutive neurogenesis in adult mouse forebrain. Nat Neurosci. 2004; 7:1233–41. [PubMed: 15494728]
9. Deng W, et al. Adult-born hippocampal dentate granule cells undergoing maturation modulate learning and memory in the brain. J Neurosci. 2009; 29:13532–42. [PubMed: 19864566]
10. Singer BH, et al. Compensatory network changes in the dentate gyrus restore long-term potentiation following ablation of neurogenesis in young-adult mice. Proc Natl Acad Sci U S A. 2011; 108:5437–42. [PubMed: 21402918]
11. Snyder JS, et al. Adult hippocampal neurogenesis buffers stress responses and depressive behaviour. Nature. 2011; 476:458–61. [PubMed: 21814201]
12. Bao S, et al. Stem cell–like glioma cells promote tumor angiogenesis through vascular endothelial growth factor. Cancer Res. 2006; 66:7843–7848. [PubMed: 16912155]
13. Liu C, et al. Mosaic analysis with double markers reveals tumor cell of origin in glioma. Cell. 2011; 146:209–21. [PubMed: 21737130]
14. Clarke MF, et al. Cancer stem cells--perspectives on current status and future directions: AACR Workshop on cancer stem cells. Cancer Res. 2006; 66:9339–44. [PubMed: 16990346]
15. Boiko AD, et al. Human melanoma-initiating cells express neural crest nerve growth factor receptor CD271. Nature. 2010; 466:133–7. [PubMed: 20596026]
16. Ishizawa K, et al. Tumor-initiating cells are rare in many human tumors. Cell Stem Cell. 2010; 7:279–82. [PubMed: 20804964]

17. Kelly PN, et al. Tumor growth need not be driven by rare cancer stem cells. Science. 2007; 317:337. [PubMed: 17641192]
18. Quintana E, et al. Efficient tumour formation by single human melanoma cells. Nature. 2008; 456:593–8. [PubMed: 19052619]
19. Vega CJ, Peterson DA. Stem cell proliferative history in tissue revealed by temporal halogenated thymidine analog discrimination. Nat Methods. 2005; 2:167–9. [PubMed: 15782184]

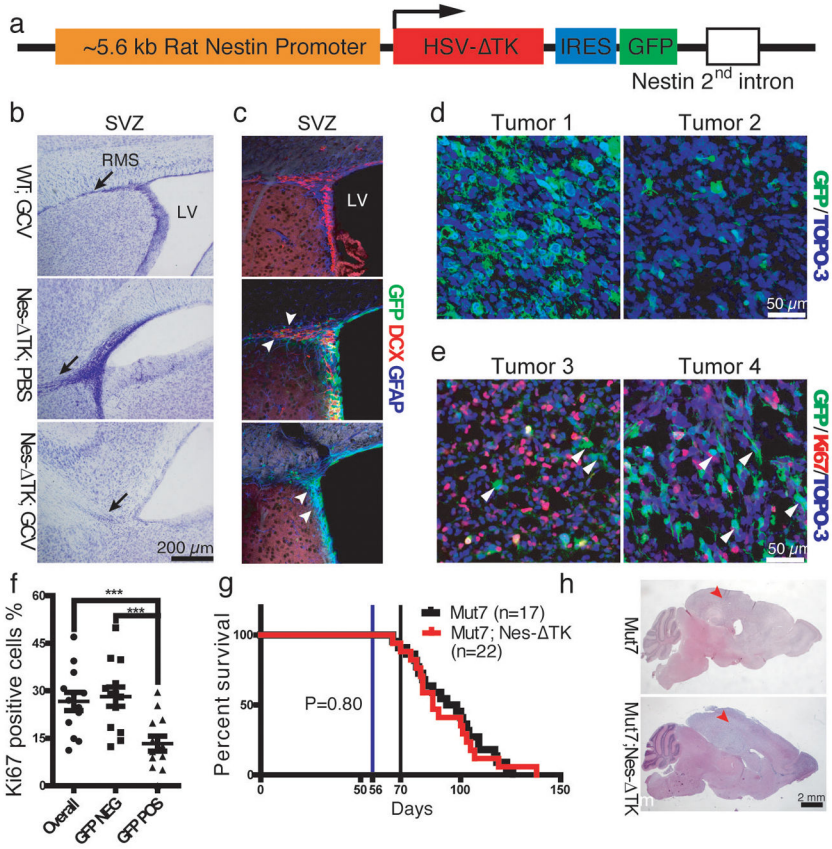

Figure 1.

Characterization of the *Nes*-Δ*TK*-*GFP* transgene. **a,** Diagram of the *Nes*-Δ*TK*-*GFP* transgene. **b,c,** GCV administration ablates neural stem cells (NSCs) in wild type mice. **b,** Representative Nissl staining of the subventricular zone (SVZ) region in wild type mice treated with GCV (WT;GCV), *Nes*-Δ*TK* transgene mice treated with PBS (*Nes*-Δ*TK*;PBS), and *Nes*-Δ*TK* transgene mice treated with GCV (*Nes*-Δ*TK*;GCV); black arrows indicate the stem cell rostral migratory stream (RMS), which is greatly reduced in the *Nes*-Δ*TK*;GCV mice. **c,** GFP (transgene), GFAP (quiescent neural stem cells) and DCX (committed neural progenitors) immunostaining of the subventricular zone (SVZ) stem cell niche. White arrowheads in middle panel (*Nes*-Δ*TK*;PBS) indicate DCX-positive GFP-negative cells more distal in the RMS. White arrowheads in bottom panel (*Nes*-Δ*TK*;GCV) indicate GFP-positive/GFAP-positive but DCX-negative quiescent NSCs. **d,** Representative GFP immunostaining in sections from two untreated gliomas of *Mut7;Nes*-Δ*TK* mice. From tumor to tumor, varying numbers of GFP-positive cells were observed. **e,** Representative GFP and Ki67 co-immunostaining in two untreated gliomas of *Mut7;Nes*-Δ*TK* mice. White arrowheads highlight GFP-positive but Ki67-negative cells, demonstrating that many transgene GFP-positive cells are quiescent. **f,** Percentage of Ki67-positive cells in GFP-positive, GFP-negative, and overall tumor population in gliomas from untreated *Mut7;Nes*-Δ*TK*-*GFP* mice. g, Kaplan–Meier survival curve of untreated *Mut7* and *Mut7;Nes*-Δ*TK* animals. No difference in percent survival was observed. **h,** Representative H&E staining of

Mut7 and *Mut7;Nes*-Δ*TK* brains without treatment. Infiltrative malignant gliomas are present in the cortex (red arrowhead) of both genotypes. *, $p<0.05$; ***, $p<0.001$.

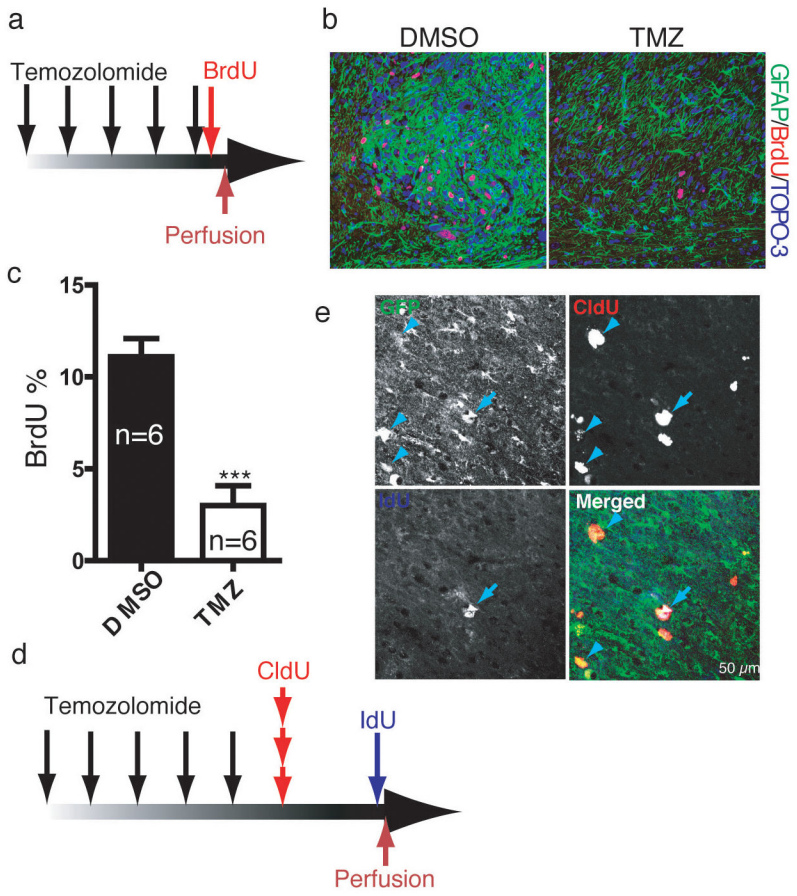

Figure 2.

TMZ targets proliferating derivatives but not the GFP+ quiescent cell population. **a,** TMZ injection schema. *Mut7* mice were treated with TMZ for five days, injected with BrdU two hours after the final TMZ treatment, and sacrificed two hours later for BrdU immunostaining. **b,** Representative GFAP/BrdU co-staining of glioma from DMSO- or TMZ-treated mice shows dramatic reduction in number of BrdU-positive cells. **c,** Quantification of the percentage of maximal BrdU-positive cells in gliomas from *Mut7* mice treated with or without TMZ showed a significant decrease in the TMZ-treated mice. (Data are mean ± s.e.m.; N=6 for each treatment; $p<0.001$.) **d–f**, *Nes*-Δ*TK*-positive cells are resistant to TMZ and produce new tumor cells. **d,** Schema of TMZ treatment and short-term labeling with BrdU analogs. *Mut7;Nes*-Δ*TK* mice were treated with TMZ for 5 days and then injected with the BrdU analogs CldU and IdU, one and three days after the last TMZ treatment, respectively. **e,** Representative tumor section illustrating that repopulating tumor cells after TMZ treatment express the *Nes*-Δ*TK* transgene (GFP+); merged panel: CldU-incorporating (arrowhead) or IdU-incorporating (arrow) cells also express GFP driven by the *Nes*-Δ*TK* transgene. (Percentage of GFP-positive cells in the CldU-positive = 77±14; percentage of GFP-positive cells in the IdU-positive population = 83±10. N=5.) Note that the majority of CldU-positive cells and IdU-positive cells are positive for GFP expression, and also that the majority of IdU-positive cells are CldU-positive, indicating the CldU-positive cells gave rise to the IdU-positive cells. ***$p<0.001$. Student's t-test.

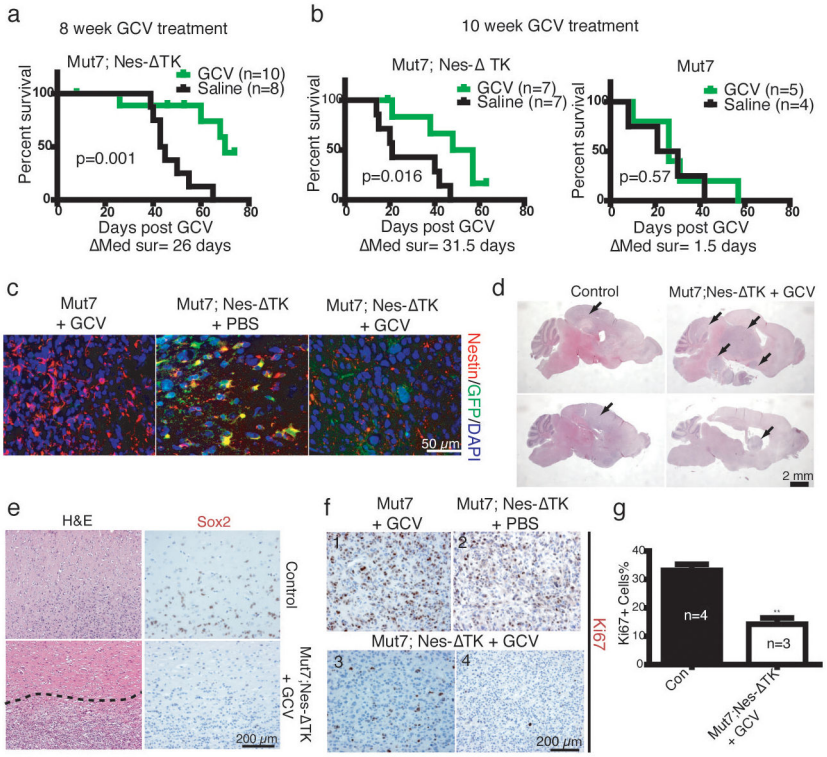

Figure 3.

GCV treatment prolongs survival of *Mut7;Nes-ΔTK* mice. **a,** Kaplan–Meier curve of *Mut7;Nes-ΔTK* mice treated with Saline or GCV for 10 weeks starting at 8 weeks of age showed a clear survival advantage for the GCV-treated mice (n=10 for GCV-treated; n=8 for saline-treated; P values determined using Log-rank test). **b,** Kaplan–Meier survival curves of *Mut7;Nes-ΔTK* (left) or *Mut7* (right) mice treated with GCV or Saline for 2 months starting at 10 weeks of age. GCV treatment increased survival of *Mut7;Nes-ΔTK* mice compared to saline treatment but had no such effect on the *Mut7* mice. (n=5–7 for the GCV-treated mice; n=4–7 for the saline-treated mice; P values determined using Log-rank test) **c,** GFP/Nestin co-immunostaining of gliomas from control (*Mut7* mice treated with GCV or *Mut7;Nes-ΔTK* mice treated with PBS) and GCV-treated *Mut7;Nes-ΔTK* mice. Elimination of GFP and nestin double-positive cells in the *Mut7;Nes-ΔTK* mice treated with GCV from 10 weeks. **d,** Representative H&E staining of control and GCV-treated *Mut7;Nes-ΔTK* brains. The tumors in the GCV-treated *Mut7;Nes-ΔTK* mice are less infiltrative than in control. Tumors indicated by black arrows. **e,** Representative H&E and Sox2 staining of tumor edges in control and GCV-treated *Mut7;Nes-ΔTK* tumors showing the GCV-treated tumors have a defined boundary (dotted line) and lack infiltrative Sox2+ cells. **f,g,** GCV treatment decreases proliferation index in *Mut7;Nes-ΔTK* tumors. **f,** Representative Ki67 staining of control (panels 1 and 2) or GCV-treated *Mut7;Nes-ΔTK* tumors (panels 3 and 4) showing the dramatic decrease in proliferation in the GCV-treated *Mut7;Nes-ΔTK* tumors. **g,** Quantification of the percentage of Ki67-positive cells in tumor regions with highest number of proliferating cells in cortex. The percentage is significantly

decreased in GCV-treated *Mut7;Nes-ΔTK* mice (n=3) versus control (n=4). Data are mean ± s.e.m.; **p<0.01. Student's t-test.

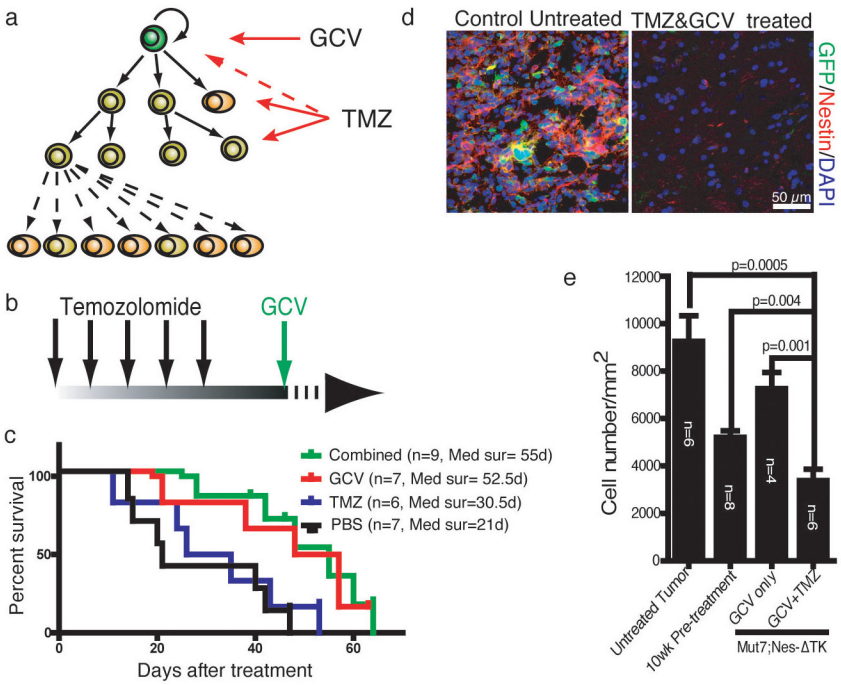

Figure 4.

Combination treatment of Temozolomide (TMZ) and GCV inhibits glioma progression in cerebrum. **a,b,** Therapeutic schema targeting both CSCs and their proliferating progeny. *Mut7;Nes-ΔTK* mice were treated with TMZ for 5 days, followed two days after by GCV. **c,** Kaplan–Meier survival curve of *Mut7;Nes-ΔTK* mice with different treatments. GCV-treated (n=7; median survival=55 days) and combinationally-treated (n=9; median survival=52.5 days) *Mut7;Nes-ΔTK* mice had similar survival advantage over TMZ-treated (n=6; median survival=30.5 days) or PBS-treated (n=7; median survival=21 days) mice. P values determined using Log-rank test. **d,** GFP and Nestin double immunostaining of vestigial tumors in TMZ/GCV-treated *Mut7;Nes-ΔTK* mice (right panel) versus tumor in control (left panel) demonstrates depletion of CSCs as evidenced by lack of GFP expression. **e,** Maximal cell density in cortical tumors with different treatment regimens. Untreated *Mut7* mice (n=6) were used as control. Tumor density of 10-week-old non-symptomatic *Mut7* mice (pre-treatment) (n=8) was used as a reference starting point. Cell density was significantly lower in the combinationally-treated (TMZ+GCV) *Mut7;Nes-ΔTK* mice (n=6) compared to untreated tumors (p=0.0005), compared to tumors in “pre-treatment” mice (p=0.004), and compared to tumors from mice treated with GCV only (n=4) (Data are mean ± s.e.m.; p=0.001; P values determined using Student’s t-test.).